TẠP CHÍ KHOA HỌC VÀ CÔNG NGHỆ ĐẠI HỌC DUY TÂN
DTU Journal of Science and Technology 01(68) (2025) 3-15

ĐẠI HỌC DUY TÂN
DUYTAN UNIVERSITY

Hybrid propulsion based on fuel cells

Động cơ hybrid dùng pin nhiên liệu

Vu Duong[a,b*], Nguyen Ha Hiep[c]
Vũ Dương[a,b*], Nguyễn Hà Hiệp[c]

[a]*School of Engineering and Technology, Duy Tan University, Da Nang, 550000, Vietnam*
[a]*Trường Công nghệ và Kỹ thuật, Đại học Duy Tân, Đà Nẵng, Việt Nam*
[b]*Institute of Research and Devolopment, Duy Tan University, Da Nang, 550000, Vietnam*
[b]*Viện Nghiên cứu và Phát triển Công nghệ cao, Đại học Duy Tân, Đà Nẵng, Việt Nam*
[c]*Institute of Vehicle and Energy Engineering, Le Quy Don Technical University, Hanoi, 100000, Vietnam*
[c]*Viện Kỹ thuật Xe và Năng lượng, Đại học Lê Quý Đôn, Hà Nội, Việt Nam*

(Date of receiving article: 23/05/2024, date of completion of review: 12/06/2024, date of acceptance for posting: 30/09/2024)

Abstract

Remotely operated vehicles (ROVs) and autonomous underwater vehicles (AUVs) have many applications in underwater missions. The problem is the power source that provides them with stable operation, especially air-independent propulsion sources such as electric batteries, accumulators, and fuel cells, to increase diving depth, underwater endurance, and range. The article mentions a different solution: to use both main energy sources simultaneously, fuel cells and batteries. The subject of the study is Pluto Plus ROVs, which are underwater vehicles for mine sweeping and counter-terrorism. The research method is simulation using MatLab Simulink against theoretical calculations to build a fuel cell model. The result was a block diagram that simulates a "hybrid" propulsion system for submersibles in general and serves as the basis for improving the propulsion system for Pluto Plus ROVs.

Keywords: Fuel cell; battery; propulsion; simulation; calculation; hybrid propulsion system.

Tóm tắt

Tàu không người lái điều khiển từ xa (ROV) và tàu lặn tự điều khiển (AUV) có nhiều ứng dụng trong các nhiệm vụ dưới nước. Vấn đề là nguồn năng lượng cung cấp cho chúng hoạt động ổn định, đặc biệt là các nguồn đẩy độc lập với không khí như pin điện, ắc quy và pin nhiên liệu, để tăng độ sâu lặn, độ bền dưới nước và phạm vi. Bài báo đề cập đến một giải pháp khác: sử dụng đồng thời cả hai nguồn năng lượng chính, pin nhiên liệu và pin. Đối tượng nghiên cứu là Pluto Plus ROVs, là phương tiện dưới nước để quét mìn và chống khủng bố. Phương pháp nghiên cứu là mô phỏng sử dụng MatLab Simulink dựa trên các tính toán lý thuyết để xây dựng mô hình pin nhiên liệu. Kết quả là một sơ đồ khối mô phỏng hệ thống đẩy "lai" cho tàu lặn nói chung và làm cơ sở để cải thiện hệ thống đẩy cho POV Pluto Plus.

Từ khóa: pin nhiên liệu; pin; lực đẩy; mô phỏng; tính toán; hệ thống đẩy "lai".

[*]*Corresponding author:* Vu Duong
Email: duongvuaustralia@gmail.com

1. Introduction

The underwater vehicles are an ideal solution for military, commercial, and scientific research, expanding the range of tasks from depth measurement to detecting underwater mines, etc. Unmanned underwater vehicles (UUV) or underwater drones are small underwater vehicles that operate underwater without direct human control. These include remotely operated vehicles (ROV) and autonomous underwater vehicles (AUV) that work independently according to the preset program. Some underwater vehicles operating in shallow water can use power supplied from shore or from surface ships by wires. Due to limited battery power reserves, the underwater functional endurance of diesel-electric submarines is limited. The submarine using the diesel engine must operate in snorkel mode to charge the battery. So, the probability of the submarine being detected by radar, infrared, optoelectronics, and acoustics increases [1]. For small underwater vehicles, diesel engines cannot be used as the primary source of propulsion. These vehicles often use electric propulsion systems (only batteries) or hybrid propulsion systems of batteries and fuel cells (FC) [2]. FCs are considered small in size, light in weight, and easy to handle, making them ideal for underwater vehicles. UUV/AUV is an emerging and growing market for marine suppliers. Mitsubishi developed and delivered an AUV called the Urashima in 2004 [3]. It uses the proton exchange membrane fuel cells (PEMFC) technology combined with a lithium-ion battery and is supplied with hydrogen from metal hydride storage and oxygen from an LOX reservoir. Vietnam's underwater vehicles currently use batteries as the main source of energy to operate, but compared to the original design of GayMarine's Pluto Plus, it uses a propulsion system with two main energy sources: a fuel cell and a battery. With the manufacturer's original powertrain, it is possible to increase the performance of Pluto Plus ROVs and achieve better autonomy.

A research paper [4] shows that PEMFC and solid oxide fuel cells (SOFC) can be used for UUVs. PEMFC has higher performance and operates at lower temperatures (below 100° C), and is therefore the preferred choice. The need to create highly efficient hybrid propulsion based on FC attracts a growing number of developers and researchers who work on designing and modeling hybrid propulsion systems. Research into hybrid propulsion system development can be carried out through: experimental study, analytical investigation, modeling and simulations. Experimental studies [5], [6], and [7] were performed without numerical calculations. Fabrication and testing of PEMFC prototypes for underwater vehicles is a time-consuming and expensive process. Using mathematical models for analytical studies makes evaluating phenomena in hybrid systems complex. Furthermore, adjusting input parameters to calibrate analytical results to coincide with experimental data can be difficult.

Numerical modeling and simulation play an essential role in developing hybrid propulsion systems because they help understand the impact of different components in the system on their performance and make it possible to tune the parts to have a complete system. In addition, it also supports optimizing size and mass to increase the underwater operating range and endurance of underwater vehicles [8], [9], and [10].

With the advantages of modeling and simulation work as mentioned above, as well as based on some simulation results in works [11] , and [12], the novelty of this study is to conduct modeling and simulation of fuel cell hybrid propulsion systems applied to an underwater vehicle using pure battery propulsion systems.

To resolve the task, some of the tasks that need to be done are to calculate the movement

resistance of an underwater vehicle, determine the propulsion power, and then calculate the power of the fuel cell and battery. Furthermore it is focuses on the model of the system components, such as fuel cells, batteries, and power converters, in the MatLab Simulink environment. Finally, it is required to simulate the system's working to have parameters to calibrate the model and complete the hybrid system as a basis for designing and manufacturing the actual hybrid system.

2. Methodology and calculation

2.1. Research object

The research object is Pluto Plus ROV [13], an underwater vehicle, a remote-controlled diving robotic system to locate, inspect, and clear underwater targets whose primary purpose is to search, identify, and clear bottom and mooring mines in extreme operating conditions and anti-terrorism.

The robot consists of two pressurized bodies joined together. Each body consists of two halves put together by bolts. Water tightness is ensured by the gasket rings placed between the grooves. The main fuselage consists of five propellers, rotary engines, a battery compartment, and electronic components. The front part of the diving robot includes a sensor head that is compact and can be raised and rotated at angles in horizontal and vertical planes. The main characteristics of Pluto Plus ROV are summarized in the following Tab.1

Table 1. Pluto Plus ROVs specifications [13]

Main parameters	Value	Unit
Dimensions	2250x580x770	mm
Weight	320	kg
Maximum carrying capacity	100	kg
Maximum speed	6	knot
Calculated speed	3.5	knot
Maximum diving depth	400	m
Underwater endurance at speed 6 knots	2	h

Thus, ROVs are unmanned submersible devices controlled remotely via the monitoring console, so their underwater range will be limited due to the lack of independent sources.

2.2. Calculation of power of a hybrid propulsion system

The calculation of power consumption for propulsion engines is based on viscous resistance using the viscous resistance coefficient C_V, the friction resistance coefficient C_F, and the shape factor (1 + k). C_F is determined by the formula (1) [14]:

$$C_F = \frac{0,075}{(\log Re - 2)^2} \quad (1)$$

Where: *Re* is the Reynolds Number.

$$Re = \frac{vL}{\mu}$$

Where: μ is the kinematic viscosity of seawater [m^2/s]; *L* is the length of ROV [*m*]; *v* is the calculated speed of ROV [*m/s*]

The shape coefficient that can be obtained from the Droblenkov curve for AUV with a circular cross section is expressed as the expression (2) [14].

$$(1+k) = 1 + 0,2\left(\frac{D}{L}\right) + 8\left(\frac{D}{L}\right)^2 - 10\left(\frac{D}{L}\right)^3 \quad (2)$$

Where: *D* is the diameter of ROV [*m*], taking the average width and height of the ROV.

Thus, viscous resistance is calculated by the expression (3) [14]:

$$R_V = \frac{1}{2}\rho\Omega v^2 C_V = \frac{1}{2}\rho\Omega v^2 C_F (1 + k) \quad (3)$$

Where: ρ = 1025 [kg/m^3]- density of seawater; Ω is the wet surface area of the ROV, calculated as a cylinder of diameter D and length L.

The required thrust power is calculated as the expression (4) where η_D is the propeller thrust performance:

$$N_p = \frac{vR_v}{\eta_D} \quad (4)$$

From expressions (3) and (4), we get a 3rd order curve representing the dependence of the thrust power and the forward rate of the ROV as expression (5):

$$N_p = \left[\frac{1}{2\eta_D}\rho\Omega C_F (1 + k)\right] v^3 \quad (5)$$

The inputs for calculating the required power are presented in Tab. 2:

Table 2. Input data for calculating the required power of ROV

Parameter	Value	Unit	Parameter	Value	Unit
μ	1.57.10^{-6}	m^2/s	T	0.58	m
v	3.5	*knots*	D	0.675	m
	1.543	m/s	B	0.77	m
L	2.25	m	η_D	0.4	-

Based on the data in Tab. 2 combined with equations from (1) to (5), we construct a curve showing the relationship between the required power and the travel speed of the ROV, with the nominal speed v = 3.5 knots, the power N_p = 222.7 W. When the maximum speed v_{max} = 6 knots, the power N_p = 1011 W, to ensure that the fuel cell pack can work best when calculating, we add the types of losses due to transmission, so the rated power to calculate for the battery pack is 300 W. The propulsion system of the original Pluto Plus ROV unit uses batteries powered directly from the onboard electrical system.

2.3. Original and proposed propulsion systems

As stated in Part 1, the propulsion system of GAYMARINE's Pluto Plus ROV device is equipped with a propulsion system including a fuel cell cluster and battery pack, but Vietnam's Pluto Plus ROV only uses batteries. It takes power directly from the ship's electrical system. With the propeller power supply scheme (load) (Figure 1), there are many limitations in terms of range and the self-propelled ability of the device when having to perform minesweeping tasks over a wide range. Therefore, with the model installed with a fuel cell cluster, it will limit the disadvantages of the current device, not to mention the relatively high energy conversion efficiency of PEM fuel cells [7].

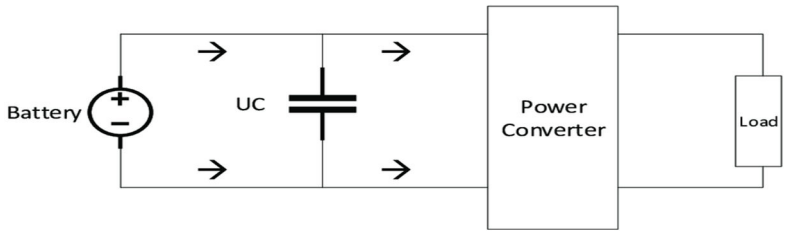

Figure 1. Power scheme for the load of the original Pluto Plus ROV

The proposed fuel cell hybrid propulsion system for the Pluto Plus ROV is shown in Figure 2. The capacity of the battery pack generated is 300 W, corresponding to the mode in which the device runs at a nominal speed of 3.5 knots. Thus, in the maximum speed mode P_{max} = 1090 W, the designed battery pack capacity accounts for about 29.6 %, and the battery will account for 70.4 % of the capacity. When the device runs below the nominal speed according to the graph in Figure 1, the power decreases (less than 300 W).

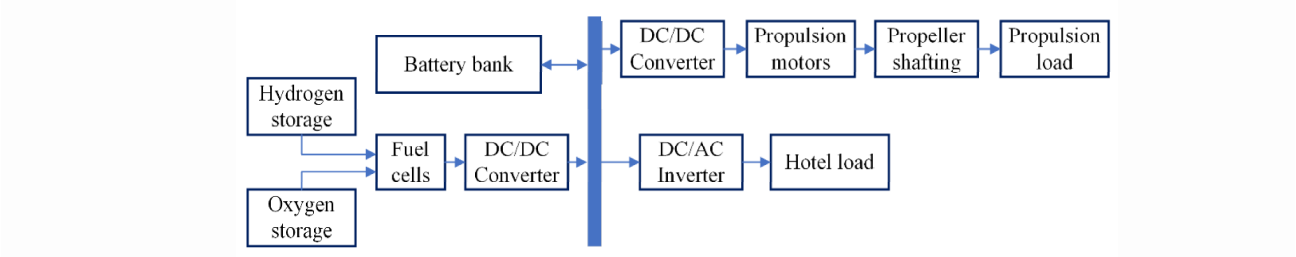

Figure 2. Proposed fuel cell hybrid propulsion system for Pluto Plus ROV

2.4. Calculating and determining fuel cell parameters

Energy is obtained in a fuel cell from thermodynamic energy through electrochemical reactions inside the fuel cell.

The energy obtained by a chemical reaction called enthalpy forms ΔH = -285.84 (kJ/mol) (which is the high calorific value when water is liquid), which is broken down into thermal energy by specific entropy ΔS (kJ/mol. K) multiplied by the absolute temperature T, and the electricity (representing the useful work of the fuel cell) is Gibbs free energy ΔG (kJ/mol). So, the total energy is [15]:

$$\Delta H = \Delta G + T.\Delta S \quad (6)$$

Where ΔG is the useful electricity determined by the amount of electricity Q (coulombs) and potential E (V):

$$W_{el} = \Delta G = -Q.E = -nFE \quad (7)$$

where n = 2 is the number of electrons transferred for each mole of fuel consumed and F is Faraday's constant (96487 C/mol) because according to Faraday's law, when electrochemically converting 1 mole of the equivalent of a substance, an electric amount flows through the system equal to Faraday's constant, and when converting 1 mole of substance, an amount of electricity flowing through the system will be equal to nF.

From this, the potential is determined as follows:

$$E = -\frac{\Delta G}{nF} = -\frac{\Delta H - T\Delta S}{nF} \quad (8)$$

This value may vary with the working temperature as well as the partial pressure of the reactants and the resulting products relative to the reference condition (T_{ref} = 25° C, P_{ref} = 1 atm). The effect of temperature changes on potential when considering ΔH and ΔS constants is calculated as follows [11]:

$$\Delta E = \frac{\Delta S}{nF}\left(T - T_{ref}\right) \quad (9)$$

From the formula (9) it shows that as the temperature increases, the potential decreases because ΔS = - 164 J/mol. K has a negative value. The partial pressure change affects ΔG because G is a function of the specific volume V (m^3/mol) and the change in pressure dP (i.e., G = V.dP). From the gas law V = RT/P, we have [15], and [11]:

$$\Delta G = \Delta G^{o} - \frac{RT}{nF} ln\left(\frac{P_{H_2}^{1} P_{O_2}^{0.5}}{P_{H_2O}^{1}}\right) \quad (10)$$

Here, ΔG_o = -237.17 kJ/mol, Gibbs free energy at standard conditions; R = 8.3143 J/mol. K is the gaseous substance constant. In the

formula (10), consider a fuel cell working on pure hydrogen with a partial pressure of P_{H2} and pure oxygen with a partial pressure of P_{O2}, knowing that to form 1 mole of water with P_{H2O} pressure (product) requires 1 mole of H_2 and 0.5 moles of O_2 (reactants), so the potential of the fuel cell [12]:

$$E_{Nerst} = -\frac{\Delta G^o}{nF} + \frac{\Delta S}{nF}(T - T_{ref}) + \frac{RT}{nF}\ln\left(\frac{p_{H_2}^1 p_{O_2}^{0.5}}{p_{H_2O}^1}\right)$$
$$= 1,229 - 0,85.10^{-3}(T - 298,15) + 4,3085.10^{-5}.T.\ln\left(\frac{p_{H_2}^1 p_{O_2}^{0.5}}{p_{H_2O}^1}\right) \quad (11)$$

Here the partial pressure values are calculated using the following formula:

$$\log p_{H_2O} = -2,1794 + 0,02953.t - 9,1837.10^{-5}.t^2 + 1,4454.10^{-7}.t^3$$

$$p_{H_2} = 0,5.\frac{P_{H_2}}{\exp\left(1,653.\frac{i_{FC}}{T^{1,334}}\right)} - p_{H_2O}$$

$$p_{O_2} = \frac{P_{O_2}}{\exp\left(4,192.\frac{i_{FC}}{T^{1,334}}\right)} - p_{H_2O}$$

The formula (11) is called the Nerst equation, which gives the maximum potential that can be achieved because there are four types of losses in fuel cells. Operational losses: this loss is necessary, like a spark, to initiate reactions. It depends on the temperature, partial pressure, and catalyst on the electrodes. Calculated by the semi-experimental formula [11]:

$$V_{act} = -\left[\xi_1 + \xi_2.T + \xi_3.T.\ln(C_{o_2}) + \xi_4.T.\ln(i_{FC})\right] \quad (12)$$

Where: ξ_i – coefficient; i_{FC} – amperage of the fuel cell [*A*]; C_{O2} - concentration of oxygen on the catalyst surface [mol/cm^3].

$$C_{O_2} = \frac{p_{O_2}}{5,08.10^6.\exp\left(-\frac{498}{T}\right)} \quad (13)$$

Om loss: this loss is due to the resistance of the proton exchange membrane (affected by the degree of membrane hydration) and the resistance due to contact between the electrode and the membrane surface as well as the electrode surface with the dipole plate and the collector plate [12].

$$V_{ohm} = i_{FC}.(R_m + R_c) \quad (14)$$

Where: R_c is the constant resistance of the cell; R_m is the temperature- dependent resistance and parameter ψ expresses the degree of membrane hydration (take a value of 14 if the membrane is fully hydrated and 23 if the membrane is oversaturated):

$$R_m = \frac{\rho_m.l}{A} \quad (15)$$

Here l – the thickness of the membrane (cm), A- the active area of the membrane (cm^2), ρ_m – the specific resistance of the membrane (Ω.cm), is determined by the formula [12]:

$$\rho_m = \frac{181,6 \cdot \left[1 + 0,03 \cdot \left(\frac{i_{FC}}{A}\right) + 0,062 \cdot \left(\frac{T}{303}\right)^2 \cdot \left(\frac{i_{FC}}{A}\right)^{2,5}\right]}{\left[\Psi - 0,634 - 3\left(\frac{i_{FC}}{A}\right)\right] \cdot \exp\left[\frac{4,18(T-303)}{T}\right]} \quad (16)$$

Concentration loss: this is called mass transfer loss; it expresses the mass transfer limit of the reactants. Although feeding reactants at high speeds will give high current densities in the fuel cell, there is a limit to the feed rate, and the reactants may not be used properly, resulting in this type of loss. Therefore, this limit is determined by the jL current density limit, which is the maximum current density value that the fuel cell can produce and is about 1.4 A/cm^2 [11], [12].

$$V_{conc} = -B \ln\left(1 - \frac{j}{j_L}\right) \quad (17)$$

where B is the coefficient depending on the cell and operating conditions, j is the instantaneous current density (A/cm2), and j = I_{FC}/A. Interference loss: this loss is caused by the interference of hydrogen and electrons passing through the membrane (electron conduction resistance); this phenomenon does not produce any useful work. The effect of this loss can be considered by adding the interferometric loss current density to the current density in the Vconc loss equations. However, interference loss current loss density is often overlooked because it has a very small value. Finally, the formula for determining the fuel cell potential is:

$$V_{cell} = E_{Nerst} - V_{act} - V_{ohm} - V_{act} \quad (18)$$

The input data to calculate the required power is shown in Table 1, and the remaining parameters of the workings of PEMFC are given in Tab. 2. The coefficients in Tab. 3 are taken from research [11] and [12]; the cathode and anode inlet pressures are taken to be 60 psig (4.08 atm) according to [7], and the proton exchange membrane is type Nafion-117. The parameters given to PEMFC are given under Tab. 3.

Table 3. Parameters for calculating PEMFC

Parameter	Value	Unit	Parameter	Value	Unit	Parameter	Value	Unit
T	353	K	B	0,08	-	ζ_3	$7,4.10^{-5}$	-
A	60	cm^2	ζ_1	-0,96	-	ζ_4	$-1,8.10^{-4}$	-
l	178.10^{-4}	cm	ζ_2	$3,12 .10^{-3}$	-	ψ	23	-
P_{H2}	3	atm	Rc	0,0008	Ω	-	-	-
P_{O2}	3	atm	j_L	1,4	A/cm^2	-	-	-

From formulas (6) to (18) combined with the values of Tab. 3, a cell polarization curve with V_{cell} = f(j) can be depicted. The results of fuel cell calculations are summarized in Tab. 4.

Table 4. Fuel cell pack calculation parameters

Parameter	Value	Unit
Number of single cell, n	14	*cell*
Current density, j	0,42	*A/cm2*
Fuel cell pack power, P	300	*W*
Fuel cell pack current, I	25	*A*
Fuel cell pack voltage, U	12	*V*
Single cell voltage, Vcell	0,84	*V*

Table 5. Input parameters set for fuel cells

Parameter	Value	Unit
Voltage in nominated mode; V_{nom}	12	*V*
Current in nominated mode; I_{nom}	25	*A*
Voltage at 0 (A) and 1(A); *V_0(A), V_1(A)*	28;26	*V*
Current at the end point; I_{end}	25,5	*A*
Voltage at the end point; V_{end}	11,74	*V*
Number of battery compartments, *n*	14	*cell*
Efficiency, η	0,57	-
Operating emperature, *t*	80	*℃*
Gas pressure H_2 supply; P_f	3	*bar*
Gas pressureO_2 supply; P_{Air}	3	*bar*
Percentage of H_2 gas in the container; x_H_2	1	-
Percentage of O_2 gas in the container; y_O_2	1	-
Percentage of water vapor in the air, $z\_H_2O(Air)$	0	-
Efficiency factor H_2, U_f_H2	0,8334	-
Efficiency of O_2 .U_fO2	0,5004	-

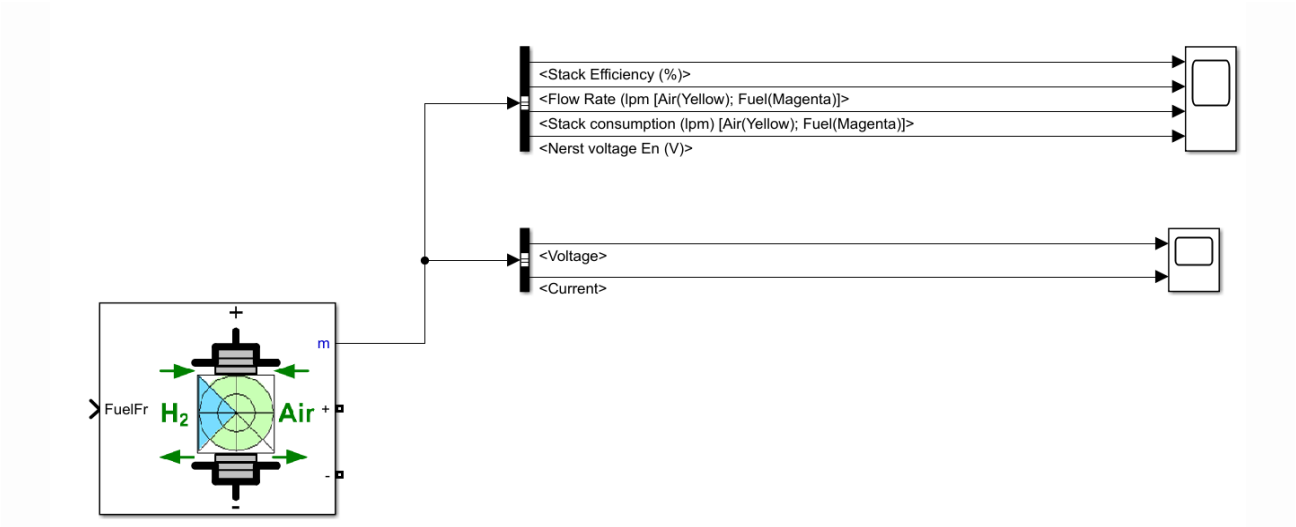

Figure 3. The PEMFC model

2.5. Modeling and simulation of a fuel cell hybrid propulsion system

The process to build a simulated block diagram for the PEMFC dynamics system goes through the following steps:

- Step 1: Build a model of the fuel cell block and set the parameters for the battery pack according to the calculated results.
- Step 2: Build a battery block model and set parameters for the battery pack.
- Step 3: Build the DC_DC Boost Converter, connect the fuel cell blocks, and calibrate the parameters. The PEMFC fuel cell block is available in Simulink, so we just need to call it out with the command “Fuel Cell Stack”. In the “block parameters”, we enter the initial

parameters for the battery according to Tab. 5. The PEMFC model is shown in the Figure 3. The battery bank of the Pluto Plus replaced in Simulink is the "Batteries" block (Figure 4). The necessary parameters for Pluto Plus are selected in accordance with the voltage generated by the fuel cell pack to ensure the battery charging process is efficient. The batteries chosen here are lead-acid batteries because they are popular on the market and are cheap and easy to maintain when needed.

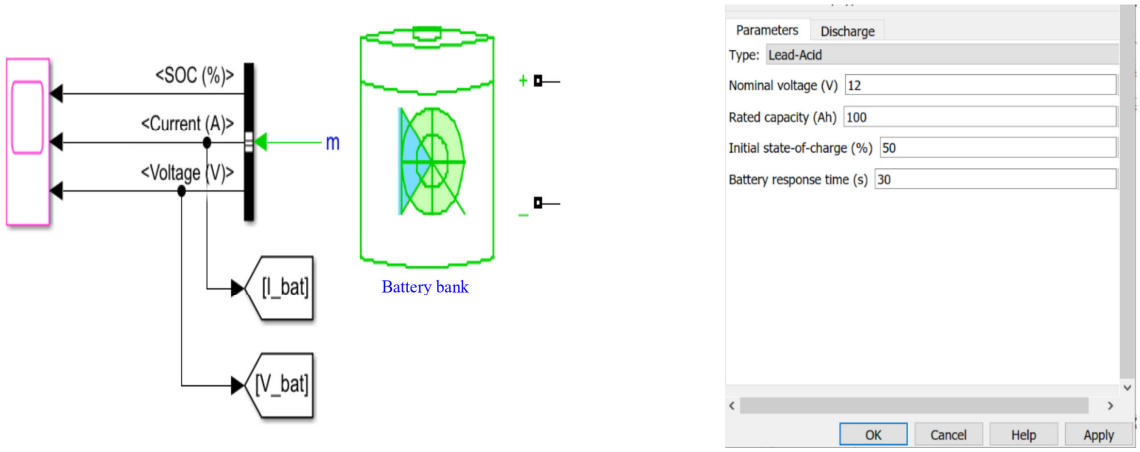

Figure 4. Block "Batteries" and input parameters set for the battery bank

As mentioned, the boost converter DC_DC is important for fuel cell propulsion by ensuring the right voltage supply to electric motors while ensuring a minimum number of battery compartments and batteries that ensure a light powertrain mass for ROVs. The turbocharger has important elements: inductors, capacitors, Mosfet-type transistors, diots, and a collapsible controller for Mosfets. The Mosfet collapsible controller used is a Proportional Integral (PI) controller based on the principle of comparing the set value with the actual value to control the pulse width to change accordingly to keep the output voltage value constant. The setting parameters for PI controllers are given in Tab. 6.

Table 6. PI controller parameters

Parameter	**Value**	**Unit**
Inductance, L	$500.e^{-6}$	H
Capacitor capacitance, C	$7500.e^{-5}$	F
Table 3.2. PI controller parameters, r	0,2	Ω
Transferring function, $G(s)$	$\frac{1}{0,0001+1}$	-
Coefficient K_P	0,005	-
Cofficient K_I	0,15	-
Voltage set, U_{ref}	24	V
Duty cycle, T_s	$1.e^{-4}$	s

To ensure the limitation of complexity in the simulation model, the whole DC_DC Boost Converter after construction is reduced to a "Subsystem" subsystem located in the block

diagram of the whole program (Figure 5). The values of the coefficients of the PI are selected based on trial and error (i.e., repeated experimentation to produce the desired result).

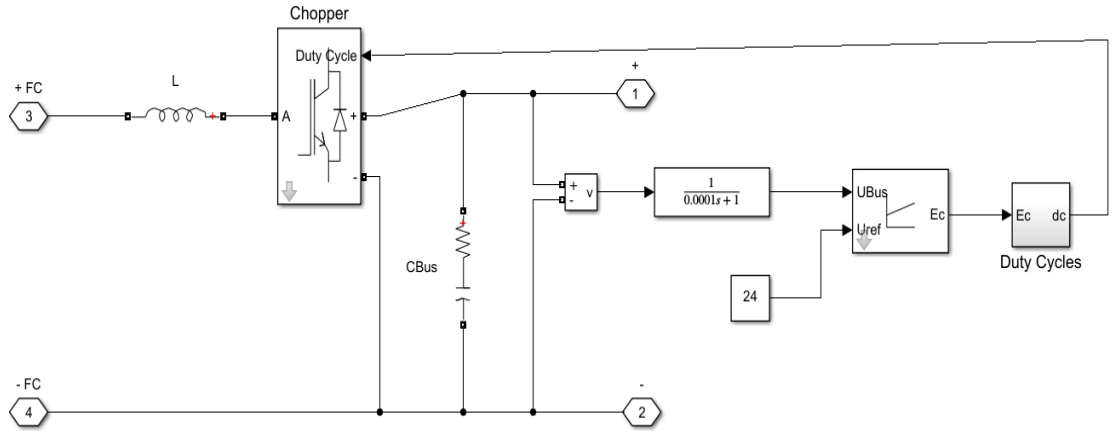

Figure 5. DC_DC boost converter built in Simulink

The load construction for the ship propulsion system is a complex system, especially the propeller electric drive system, so to make it simpler for the simulation process, we use resistor blocks instead of load assemblies (from hybrid electric motors to propellers). The goal from the beginning was to see the interaction of three power components: load capacity (P_R), fuel cell assembly capacity (PFC), and battery pack capacity (P_{Bat}). In which the capacity of the PEM fuel cell pack is designed with a constant power from the beginning of 300W, corresponding to a rated rate of 3.5 knots. With a "hybrid" type propulsion system consisting of both fuel cell and battery clusters that together supply energy to the load, below the rated value, the fuel cell assembly simultaneously performs two tasks: supplying power to the load and charging the battery pack ($P_{FC} = P_{Bat} + P_R$); in higher-than-rated speed mode, now both the fuel cell assembly and the battery of the Pluto Plus ROVs supply power to the load, ensuring the effective voltage value output for the propeller hybrid motorcycle ($P_{FC} = P_R + P_{Bat}$). To show this change, the P_R must change within the preset simulation period (10 seconds), and specifically for this change, the load capacity must increase. With a fixed output voltage of 24 volts, for the power to increase, the resistance must decrease. It is assumed here that the law of reduction of load resistance over time is given by Equation. $R(t) = -0{,}5231559633\ .t + 5{,}76$.

In Simulink, a rheostat is called a "Variable resistor" block, with the input "R" being the law of change of the rheostat. To build the law of transformation for input "R", it is necessary to add blocks "Fcn" and "Clock". The model of a rheostat is shown in Figure 6.

After building all the parts: fuel cell assembly, battery pack, load, connect these parts, and let the program start running according to the pre-established simulation time, In addition to the main blocks built and set parameters, to display simulation results, there are other blocks such as the "Product" block to multiply the voltage and current values to give the power value, the "Display" block to display the values, the "Scope" block to display the results in the form of graphs according to the simulation time, and the special block. After building all the blocks, run the simulation on Simulink by pressing the keyboard shortcut "Ctrl + T" or pressing the "RUN" icon on the toolbar in Simulink.

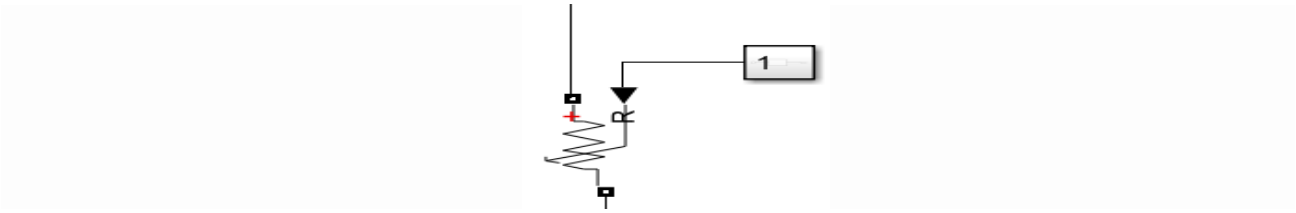

Figure 6. Model of a rheostat

Once the program is running, the software will check the program for errors and then run the results. The block diagram of the complete simulation is shown in Figure 7.

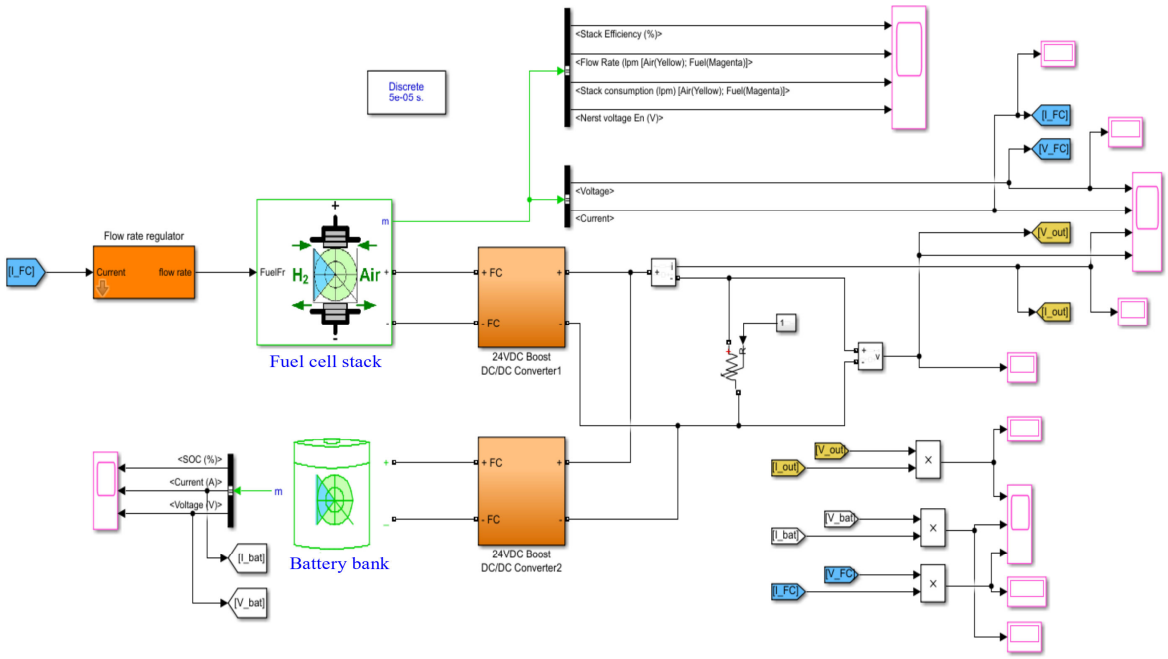

Figure 7. Fuel cell hybrid propulsion system

3. Results and discussion

The result of running the simulation is shown as a simulation time-dependent graph in the "Scope" block. Output the program's simulation results through the three set scope screens (Figures 8-9). In addition, the "Display" displays will show the stability parameters of the values we need to output; these values show us the stable value of the block diagram compared to the set value. In addition to the simulation results built from the block diagram in Simulink, some other results for the fuel cell assembly are written in the MatLab programming section to see the relationship between fuel cell parameters when operating.

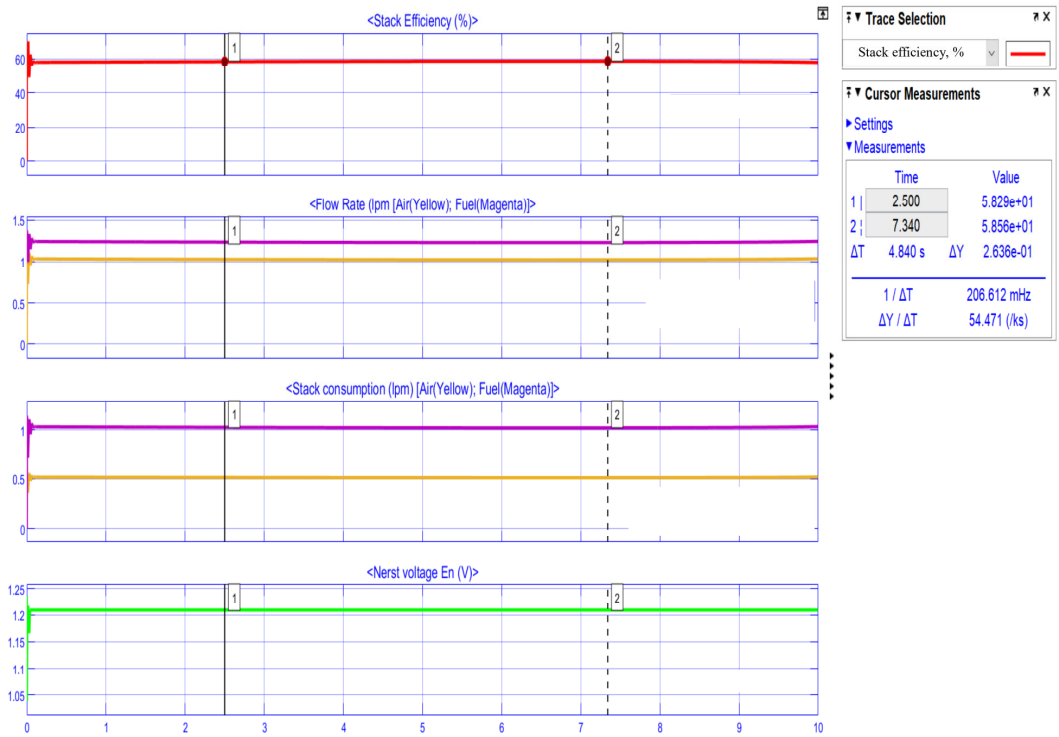

Figure 8. Simulation results of PEMFC operating parameters

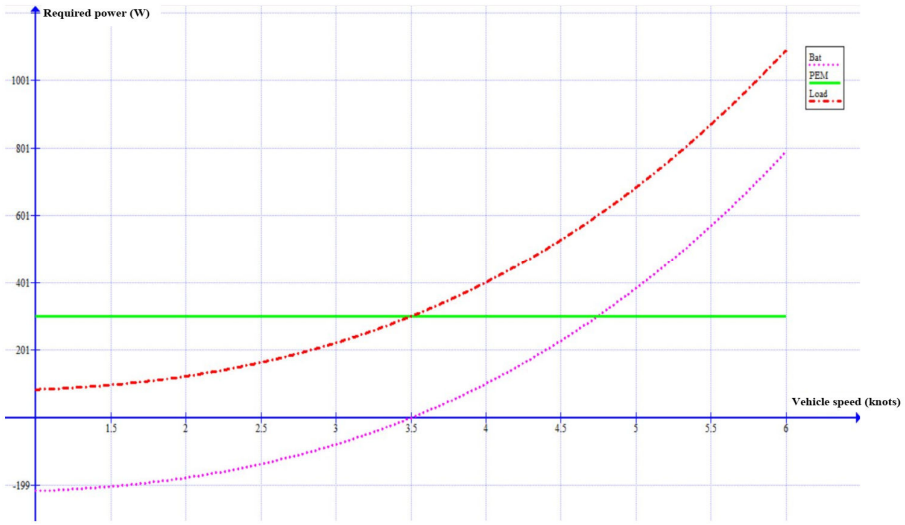

Figure 9. Simulation of power depends on operating ROV speeds

According to Figure 9, the voltage and current of PEMFC are relatively stable at 12 V and 25 A, while the voltage drop on the propeller hybrid engine is also stable at 24 V. The change in load according to the vessel propulsion power is the change in the upper current applied to the electric motor. When the ROV speed changes, the values may change slightly but not significantly, which can be considered.

4. Conclusion

Calculations were done on several key components of the fuel cell hybrid propulsion system, including the fuel cell stack, battery bank, fuel flow rate, humidifier calculation, Boost Converter DC_DC, and Rheostat. Hybrid propulsion for Pluto Plus ROVs may be simulated utilizing proton-to-battery exchange membrane fuel cell assemblies. A block diagram was created mimicking the powertrain of Pluto

Plus ROVs after adding a fuel cell assembly, using MatLab Simulink and previously computed and defined parameters. The simulation findings revealed the importance of the proton exchange membrane fuel cell (PEMFC) in the overall propulsion system. This finding may be regarded a preliminary perspective of the entire "hybrid" propulsion system for submersibles in general, as well as the foundation for enhancing the propulsion system for the present Pluto Plus ROVs to satisfy numerous needs.

References

[1] Lee, Jen-Chieh and Shay, Tony. (2018). "Analysis of fuel cell applied for submarine air independent propulsion (AIP) system". *Journal of Marine Science and Technology*. Vol. 26: Iss. 5, Article 5. DOI: 10.6119/JMST.201810_26(5).0005.

[2] Van Biert L., M. Godjevac, K. Visser and P.V. Aravind. (2016). A review of fuel cell systems for maritime application. *Journal of Power Sourses*. 327, 345-364 (2016). http://dx.doi.org/10.1016/j.jpowsour.2016.07.007.

[3] W. Winkler. (2009). *Applications - transportation, ships: Fuel Cells*. Encyclopedia of Electrochemical Power Sources. Elsevier, pp.338-358, ISBN 9780444527455, https://doi.org/10.1016/B978-044452745-5.00340-3.

[4] Carrette, L, Friedrich, K A, and Stimming, U. (2001). *Fuel cells - fundamentals and applications*. Germany: N. p., 2001. Web. doi:10.1002/1615-6854(200105)1:1<5::AID-FUCE5>3.0.CO;2-G.

[5] Helge Weydahl, Martin Gilljam, Torleif Lian, Tom Cato Johannessen, Sven Ivar Holm, Jon Øistein Hasvold. (2020). "Fuel cell systems for long-endurance autonomous underwater vehicles – challenges and benefits, International". *Journal of Hydrogen Energy*. Volume 45, Issue 8, 2020, Pages 5543-5553, ISSN 0360-3199, https://doi.org/10.1016/j.ijhydene.2019.05.035.

[6] Nai-Chien Shih, Biing-Jyh Weng, Jiunn-Yih Lee, Yung-Chia Hsiao. (2013). "Development of a small fuel cell underwater vehicle, International". *Journal of Hydrogen Energy*. Volume 38, Issue 25, Pages 11138-11143, ISSN 0360-3199, https://doi.org/10.1016/j.ijhydene.2013.01.095.

[7] Nai-Chien Shih, Biing-Jyh Weng, Jiunn-Yih Lee, Yung-Chia Hsiao. (2014). "Development of a 20 kW generic hybrid fuel cell power system for small ships and underwater vehicles, International". *Journal of Hydrogen Energy*. http://dx.doi.org/10.1016/j.ijhydene.2014.01.113.

[8] Mohamed M. Albarghot, Mohamed T. Iqbal, Kevin Pope, Luc Rolland. (2020). "Dynamic modeling and simulation of the MUN Explorer autonomous underwater vehicle with a fuel cell system[J]. *AIMS Electronics and Electrical Engineering*. 4(1): 114-131. doi: 10.3934/ElectrEng.2020.1.114.

[9] Nguyen Ha, H., Nguyen Quoc, Q., & Cu Xuan, P. (2022). "Early-Stage analysis of air independent propulsion based on fuel cells for small submarines". *Advances in Military Technology*. 17(2), 457–469. https://doi.org/10.3849/aimt.01744.

[10] De Lorenzo, G.; Piraino, F.; Longo, F.; Tinè, G.; Boscaino, V.; Panzavecchia, N.; Caccia, M.; Fragiacomo. (2022). "P. Modelling and performance analysis of an autonomous marine vehicle powered by a fuel cell Hybrid powertrain". *Energies 15*, 6926. https://doi.org/10.3390/en15196926.

[11] Saeed, E. W., & Warkozek, E. G. (2015). "Modeling and analysis of renewable PEM fuel cell system". *Energy Procedia, 74, 87–101*. doi:10.1016/j.egypro.2015.07.527.

[12] Ansari, S. A., Khalid, M., Kamal, K., Abdul Hussain Ratlamwala, T., Hussain, G., & Alkahtani, M. (2021). "Modeling and simulation of a proton exchange membrane fuel cell alongside a waste heat recovery system based on the organic rankine cycle in MatLab/Simulink environment". *Sustainability, 13(3), 1218*. doi:10.3390/su13031218.

[13] Pluto Plus, Pluto and Pluto-L-medium size minehunting ROVs: http://www.idrobotica.com/pluto-plus.php.

[14] D' Amore-Domenech, R., Raso, M. A., Villalba-Herreros, A., Santiago, Ó., Navarro, E., & Leo, T. J. (2018). "Autonomous underwater vehicles powered by fuel cells: Design guidelines". *Ocean Engineering, 153, 387–398*. doi:10.1016/j.oceaneng.2018.01.117.

[15] EG&G technical services. (2004). Inc. *In Fuel Cell Handbook*. 7th ed.; US Department of Energy, Office of Fossil Energy, National Energy Technology Laboratory: Morgantown, WV, USA.